

The stress field for a screw dislocation near cavities and straight boundaries

V.A. Lubarda*, X. Markenscoff

Department of Mechanical and Aerospace Engineering, University of California, 9500 Gilman Drive San Diego, La Jolla, CA 92093-0411, USA

Received 25 June 2002; received in revised form 18 October 2002; accepted 22 October 2002

Abstract

The stress distribution and dislocation forces for screw dislocations near cavities and straight boundaries are examined, depending on the selected cut used to impose a displacement discontinuity and create a dislocation. The location of the equilibrium dislocation position is determined in each considered case. The slip-induced stress amplification in thin ligaments between a cavity and a straight boundary, between the inner and outer surface of an eccentric hollow cylinder, and between two approaching cavities in an infinite medium are calculated. It is shown that in the limit of vanishingly small ligament width d , the shearing stress amplifies at the order of $d^{-1/2}$.

© 2002 Elsevier Science B.V. All rights reserved.

Keywords: Cavities; Dislocations; Free Surfaces; Ligaments; Slip; Stress amplification

1. Introduction

The stress and strain fields, the strain energy, and dislocation forces for a screw or edge dislocation in a simply-connected region do not depend on the cut along which a displacement discontinuity is imposed. Only displacements differ in the regions between different cuts by a rigid-body translation. The situation is different for multiply connected regions, where the solution depends on the cut used to create a dislocation, and if the connectivity of the region is n , there are as many possible solutions. This was demonstrated in Ref. [1] for a screw dislocation in a hollow cylinder and near a cavity in an infinite body. The results are here extended to other cases of interest. A detailed analysis is given for a screw dislocation between a cavity and a free surface of a half-space, and for a screw dislocation between two cavities in an infinitely extended material. Two different solutions are derived in the former case, and three in the latter case. The method of image dislocations is conveniently used to obtain these solutions. The results are

then applied to study a slip-induced stress amplification in thin ligaments between a cavity and a free surface of a half-space, between inner and outer surfaces of an eccentric hollow cylinder, and between two approaching cavities in an infinite space. The presented analysis extends the earlier analysis of stress amplification in vanishingly small geometries by Markenscoff [2], and Wu and Markenscoff [3]. In particular, it is shown that in the limit of vanishingly small ligament width d , the shearing stress amplifies at the order of $d^{-1/2}$.

The solution for a screw dislocation at a distance h from a free surface of a half-space $y = 0$ is obtained by summing the solutions for a dislocation at the point $(0, h)$ and an image dislocation of the opposite sign at the conjugate point $(0, -h)$ within an infinite space. The two dislocations cancel each other's traction over the surface $y = 0$ and provide the solution for a screw dislocation in a half-space. The solution for a screw dislocation eccentrically situated in a circular cylinder was derived by Eshelby [4]. If a screw dislocation is at a distance a from the center of a cylinder of radius R , there is an image dislocation of opposite sign at the conjugate point at distance R^2/a from the center. The two dislocations cancel each other's stress fields on the cylindrical surface $r = R$. Eshelby also considered the end effects in the case of a cylinder of finite length, and the resulting con-

* Corresponding author. Tel.: +1-858-453-8053; fax: +1-858-453-5698.

E-mail address: vlubarda@uscd.edu (V.A. Lubarda).

sequences on the location of the equilibrium dislocation position. Previously, Eshelby and Stroh [5] obtained the solution for a screw dislocation at the center of a short disk, accounting for the traction free boundary conditions on all sides of the disk.

A study of edge dislocations in plane strain is more difficult, because the method of image dislocations is not sufficient to achieve the traction free boundary conditions (e.g., Nabarro [6], Hirth and Lothe [7]). Equilibrium distributions of edge dislocations near stress-free boundaries were recently studied analytically and numerically in [8–13]. The results for slip-induced stress amplification obtained in this paper for screw dislocations and antiplane strain can be numerically extended to the case of edge dislocations and plane strain. The analysis of more complex dislocation configurations near free boundaries, such as straight dislocations emerging at the planar surface, or straight dislocations near the spherical cavity are more complex and few analytical results are available (e.g., [14,15]).

2. Screw dislocation near a cavity within a half-space

For a screw dislocation between a cavity and a free surface of a half-space (Fig. 1), infinitely many image dislocations are needed to fulfill the traction free boundary conditions. One half of image dislocations is within the boundary of the cavity, and the other half is to the right of the free surface of a half-space. If the center of the cavity of radius R is at a distance h from the free surface, and if the dislocation is at a distance a from the center of the cavity, the shear stresses are

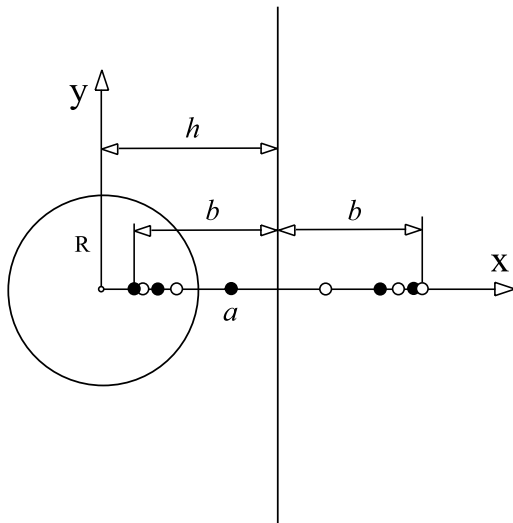


Fig. 1. A screw dislocation between a cavity and a free surface of a half-space. Image dislocations pile-up at two conjugate points at distance b from the boundary of a half-space.

$$\sigma_{zx} = -\frac{\mu b_z}{2\pi} \sum_{n=0}^{\infty} \left[\frac{y}{(x - a_{n-1})^2 + y^2} - \frac{y}{(x - a_n)^2 + y^2} + \frac{y}{(x - R^2/a_n)^2 + y^2} - \frac{y}{(x - R^2/a_{n-1})^2 + y^2} \right], \quad (1)$$

$$\sigma_{zy} = \frac{\mu b_z}{2\pi} \sum_{n=0}^{\infty} \left[\frac{x - a_{n-1}}{(x - a_{n-1})^2 + y^2} - \frac{x - a_n}{(x - a_n)^2 + y^2} + \frac{x - R^2/a_n}{(x - R^2/a_n)^2 + y^2} - \frac{x - R^2/a_{n-1}}{(x - R^2/a_{n-1})^2 + y^2} \right], \quad (2)$$

where μ is the shear modulus, and b_z is the Burgers vector of the dislocation. In these equations, the recursive formulas apply

$$a_n = 2h - b_{n-1}, \quad b_n = \frac{R^2}{a_{n-1}}, \quad n = 1, 2, 3, \dots, \quad (3)$$

with $a_0 = b_0 = a$. All image dislocations are in the region between $h - b$ and $h + b$ from the center of the cavity, where $b = (h^2 - R^2)^{1/2}$. In Eq. (1) and Eq. (2) it is implied that the displacement discontinuity is imposed along a cut from the point a to the free surface of a half-space (or from the point a to $-\infty$), as shown in Fig. 2a. If the

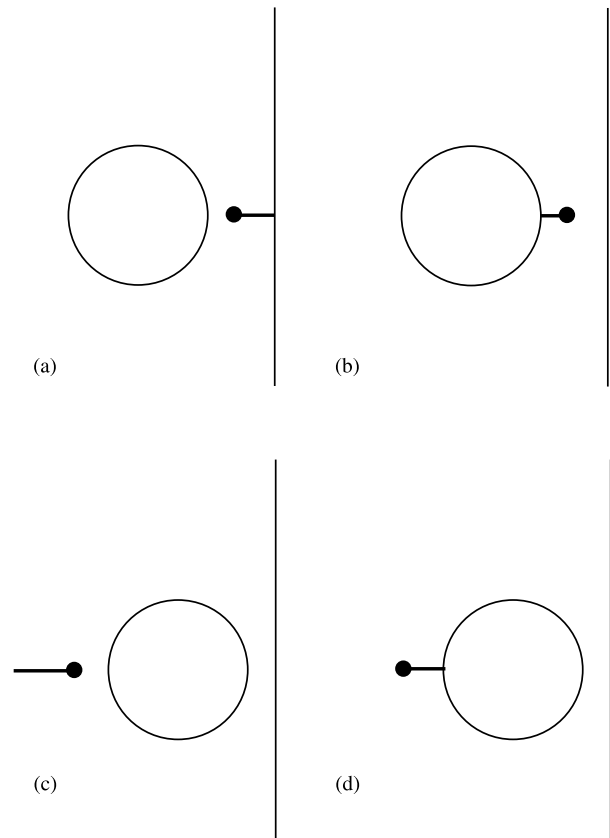


Fig. 2. Two different cuts used to create a dislocation between a cavity and a free surface of a half-space; parts (a) and (b). The same for a dislocation to the left of the cavity; parts (c) and (d).

dislocation is introduced by a displacement discontinuity along a cut from the point on the cavity to a (Fig. 2b), one needs to add to the previous solution a solution for the negative dislocation at the point $h-b$ along the x -axis, and a solution for the positive dislocation at the point $h+b$. These two dislocations are mirror image of each other in the plane $x=h$, and are also conjugate points with respect to the cavity, producing no traction on either boundary. If $h=2R$, for example, the dislocation is at an unstable equilibrium position for $a \approx 1.343R$ in the first case, and for $a \approx 1.647R$ in the second case. The latter distance is greater because when $a \approx 1.343R$ the dislocation force in the first case is directed away from the cavity, and is balanced in the second case by added pair of dislocations at two conjugate points. A somewhat more involved, but still straightforward construction of image dislocations can be used in the case when a screw dislocation is above the cavity, i.e., along the y -axis in Fig. 1. In the limit $h \rightarrow \infty$, keeping R constant, the solution for a dislocation near a cavity in an infinite body is recovered [1]. If both h and R tend to ∞ , but $h-R=d$ remains constant, the solution for a dislocation in an infinite strip of width d is obtained.

A similar analysis can be performed if the dislocation is located to the left of the cavity, at the distance a from its center (Fig. 2c). In this case one only needs to use $a_0 = b_0 = -a$ in the recursive formulas (Eq. (3)). A displacement discontinuity is imposed from $-\infty$ to $x = -a$ (or from $x = -a$ to $x = h$). If a displacement discontinuity is imposed from $x = -a$ to $x = -R$ (Fig. 2d) we add to the previous solution the solution for a negative dislocation at $x = h-b$ and a positive dislocation at $x = h+b$. A simple special case of this is obtained when $h=0$, so that the dislocation is near a semi-circular groove of a half-space. Only three image dislocations are required in this case to fulfill the traction free boundary conditions along the groove and the straight edge of a half-space.

If there is more than one dislocation within the material, the stress field is obtained by superposition of stress fields of individual dislocations. For a random distribution of dislocations, numerical evaluations are needed, as described in Ref. [9]. It is of interest to examine the mutual effect of two dislocations on the stress field of each other. For example, consider the first dislocation to be in the ligament between the cavity and the free surface, and the second dislocation to the left of the cavity. Both dislocations are created by cuts from the dislocation to the cavity. The stress field within the ligament will then be less affected by the second dislocation, closer this dislocation is to the cavity. This is so because the stress field of a pair of two opposite dislocations at small distance l decreases with the distance r as $\mu b_z l / r^2$. In the process of introducing image dislocations, l rapidly diminishes for each new

pair of dislocations, and since the first dislocation is within the ligament it makes a dominant stress contribution there. This is particularly pronounced for higher values of the ratio R/h (thin ligaments). If two dislocations are both between the cavity and the straight boundary, there is a stronger interaction of dislocations with each other, and with the free surface of the cavity and the straight boundary. If dislocations are alike, they would tend to exit the material by mutual repulsion and by the attraction from the free surfaces.

3. Screw dislocation in an eccentric hollow cylinder

The solutions for a screw dislocation between a cavity and a free surface of a half-space, and for a screw dislocation in a hollow cylinder can both be deduced by appropriate limits from a more general problem of a screw dislocation in an eccentric hollow cylinder (Fig. 3). All image dislocations outside the outer boundary of the cylinder are at the distances a_n , and all image dislocations within the inner boundary of the cylinder are at the distances b_n from the center of the inner circle, where

$$a_n = \frac{R_1^2}{c + b_{n-1}} - c, \quad b_n = \frac{R_2^2}{a_{n-1}}, \quad n = 1, 2, 3, \dots \quad (4)$$

The spacing between the centers of the two circles is c . For $n=0$, we have $a_0 = b_0 = a$. The dislocations pile up at two points, conjugate with respect to both circles, which are at

$$x_{1,2} = \frac{1}{2c} [R_0^2 \pm (R_0^4 - 4c^2 R_2^2)^{1/2}], \quad R_0^2 = R_1^2 - R_2^2 - c^2 \quad (5)$$

from the center of the inner circle. A displacement discontinuity is imposed along a cut from $x = a$ to $x = R_1 - c$ (Fig. 4a). If we add to this solution the solution for a positive dislocation at $x = x_1$ and a negative

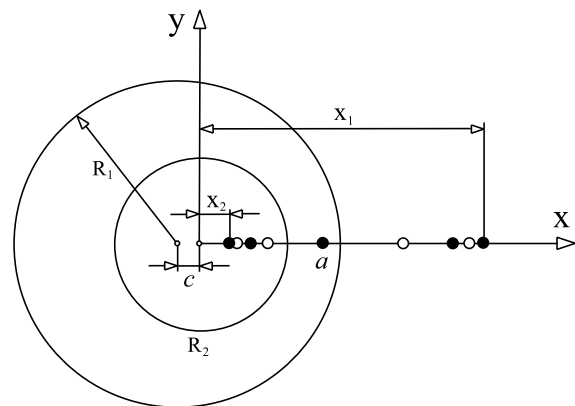


Fig. 3. Dislocation in an eccentric hollow cylinder. Image dislocations pile-up at two conjugate points at distances x_1 and x_2 from the center of the inner boundary.

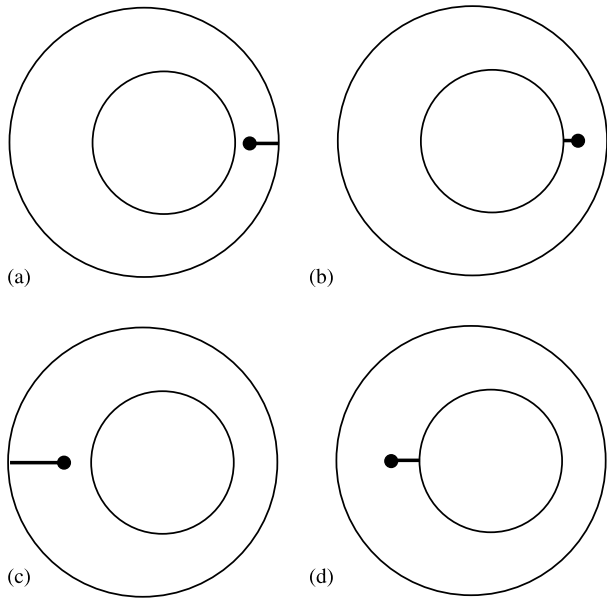


Fig. 4. Two different cuts used to create a dislocation in an eccentric hollow cylinder; parts (a) and (b). The same for a dislocation to the left of the inner boundary; parts (c) and (d).

dislocation at $x = x_2$, the solution for a cut shown in Fig. 4b is obtained. If a dislocation is to the left of the inner circle (Fig. 4c), we use $a_0 = b_0 = -a$ in the recursive formulas Eq. (4). By adding to this solution the solution for a positive dislocation at $x = x_1$ and a negative dislocation at $x = x_2$, the solution for a cut shown in Fig. 4d is deduced. If $R_1 - c \rightarrow h$, while both R_1 and c become infinitely large, we recover the result $a_n = 2h - b_{n-1}$ for a screw dislocation near the cavity in a half-space.

From an alternative standpoint, the solution for a screw dislocation in an eccentric hollow cylinder can be obtained from the solution for a dislocation in a concentric hollow cylinder by using the mapping of an eccentric into a concentric annulus. The conformal mapping is particularly important in the cases when the image method does not work, e.g., when in the process of introducing image dislocations, some of them fall within the region of actual material (Seeger [16]).

4. Screw dislocation between two cavities in an infinity body

Consider a screw dislocation between two cavities in an infinite medium. The radii of the cavities are R_1 and R_2 , and their distance is c (Fig. 5). Two infinite sets of image dislocations are required to achieve the traction free conditions on the surfaces of both cavities. One set of image dislocations is entirely within the region of the first cavity, and the other is entirely within the region of the second cavity.

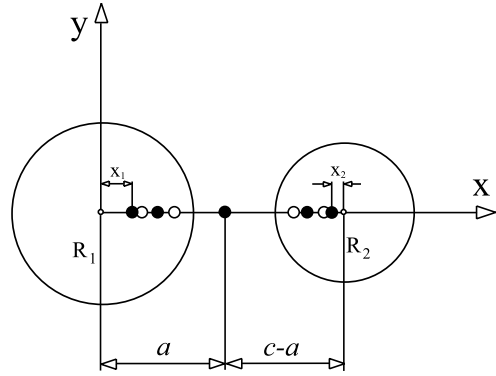


Fig. 5. Screw dislocation between two cavities in an infinite medium. Image dislocations pile-up at two conjugate points at distances x_1 and x_2 from the centers of two cavities.

The stresses are consequently

$$\sigma_{zx} = -\frac{\mu b_z}{2\pi} \times \left\{ \frac{y}{(x-a)^2 + y^2} + \sum_{n=1}^{\infty} \left[\frac{y}{(x-b_{2n})^2 + y^2} - \frac{y}{(x-a_{2n-1})^2 + y^2} + \frac{y}{(x-c+a_{2n})^2 + y^2} - \frac{y}{(x-c+b_{2n-1})^2 + y^2} \right] \right\}, \quad (6)$$

$$\sigma_{zy} = \frac{\mu b_z}{2\pi} \times \left\{ \frac{x-a}{(x-a)^2 + y^2} + \sum_{n=1}^{\infty} \left[\frac{x-b_{2n}}{(x-b_{2n})^2 + y^2} - \frac{x-a_{2n-1}}{(x-a_{2n-1})^2 + y^2} + \frac{x-c+a_{2n}}{(x-c+a_{2n})^2 + y^2} - \frac{x-c+b_{2n-1}}{(x-c+b_{2n-1})^2 + y^2} \right] \right\} \quad (7)$$

The recursive formulas

$$a_{2n} = \frac{R_2^2}{c - a_{2n-1}}, \quad a_{2n+1} = \frac{R_1^2}{c - a_{2n}}, \quad (8)$$

$$b_{2n} = \frac{R_1^2}{c - b_{2n-1}}, \quad b_{2n+1} = \frac{R_2^2}{c - b_{2n}}, \quad (9)$$

apply for $n = 1, 2, 3, \dots$, with $a_1 = R_1^2/a$, and $b_1 = R_2^2/(c-a)$. As n goes to ∞ , the image dislocations in the first cavity pile up at the distance x_1 from its center, while the image dislocations in the second cavity pile up at the distance x_2 from the center of the second cavity. The two points are conjugate to each other with respect to both cavities, and are thus specified by

$$c - x_2 = \frac{R_1^2}{x_1}, \quad c - x_1 = \frac{R_2^2}{x_2}. \quad (10)$$

This gives

$$x_1 = \frac{1}{2c}(c^2 - c_0^2 + R_1^2 - R_2^2), \quad (11)$$

$$x_2 = \frac{1}{2c}(c^2 - c_0^2 + R_2^2 - R_1^2),$$

where

$$c_0^4 = [c^2 - (R_1 + R_2)^2][c^2 - (R_1 - R_2)^2]. \quad (12)$$

The contributions from the pairs of positive and negative image dislocations are summed in Eq. (6) and Eq. (7), which ensures the convergence of the series, and implies a displacement discontinuity along a cut from the point a to ∞ . If $R_2 = 0.5R_1$ and $c = 2.5R_1$, for example, we find that the dislocation is at an unstable equilibrium position for $a \approx 1.535R_1$. The variation of the dislocation force, as the dislocation moves between two cavities, is shown by a solid curve in Fig. 6.

The derived solution is associated with a displacement discontinuity along a cut from the point a to ∞ . One such cut is shown in Fig. 7a. Two other solutions are, however, possible since two cavities in an infinite medium make a triply connected region. One solution corresponds to a displacement discontinuity along a cut from the point a to the surface of one cavity, and the other is associated with a cut from the point a to the surface of another cavity (Fig. 7b,c). Details are given by Markenscoff and Lubarda [17]. When a displacement discontinuity is imposed as in Fig. 7b, the dislocation force varies with the dislocation position between two cavities as shown by a dashed curve in Fig. 6. Dislocation is in an unstable equilibrium for $a \approx 1.220R_1$. If a dislocation is created by a displacement discontinuity along a cut shown in Fig. 7c, the dislocation force varies

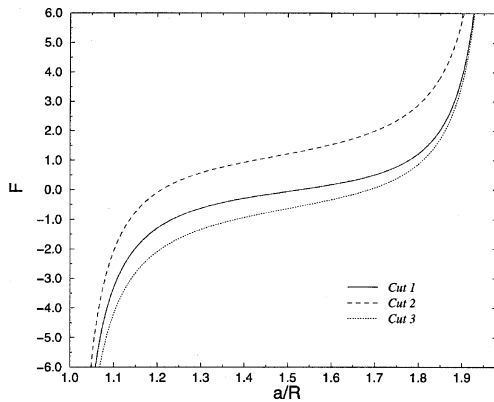


Fig. 6. The variation of dislocation force (scaled by $\mu b_z^2/2\pi R_1$) as the dislocation moves along horizontal direction between two cavities in an infinite medium. Three different curves correspond to three different ways of creating a dislocation, indicated in Fig. 7.

as indicated by a dotted curve in Fig. 6. In this case, the dislocation is in an unstable equilibrium for $a \approx 1.695R_1$.

5. Slip-induced stress amplification in thin ligaments

A comprehensive analysis of stress amplification in vanishingly small geometries due to remote stress or thermal loading was given in Refs. [2,3]. We extend their analysis in this section by presenting analytical solutions for slip-induced stress amplification in thin ligaments within multiply connected regions. The first considered case is depicted in Fig. 8. We want to calculate the stress field associated with an imposed slip discontinuity of amount b_z across the ligament of width d (or, equivalently, along a cut from $-\infty$ to the surface of the cavity). The solution is obtained by placing a negative dislocation at the point $x = h - b$ and a positive dislocation at the point $x = h + b$, where $b = (h^2 - R^2)^{1/2}$. These two dislocations are mirror image of each other in the plane $x = h$, and are also conjugate points with respect to the cavity, producing no traction on either boundary. The shear stress $\tau(x) = \sigma_{zy}(x, 0)$ across the ligament is, therefore,

$$\tau(x) = \frac{\mu b_z}{2\pi} \left(\frac{1}{x - h + b} - \frac{1}{x - h - b} \right). \quad (13)$$

Introducing a non-dimensional variable ζ such that

$$b = (1 + \zeta)R, \quad \zeta = \frac{d}{R}, \quad (14)$$

it readily follows that the shear stresses at the end points of the ligament are

$$\tau_1 = \tau(R) = \frac{\mu b_z}{2\pi R} \sqrt{2 + \zeta} \zeta^{-1/2},$$

$$\tau_2 = \tau(b) = \frac{\mu b_z}{\pi R} \frac{1}{\sqrt{2 + \zeta}} \zeta^{-1/2}. \quad (15)$$

In the limit as $\zeta \rightarrow 0$, this establishes the $\zeta^{-1/2}$ order of singularity in the region of the ligament, produced by the relative sliding of two faces of the ligament. For example, if $R = 10b_z$ and $d = b_z$ (so that $\zeta = 0.1$), there follows $\tau_1 = 0.0279\mu$ and $\tau_2 = 0.0695\mu$.

The longitudinal displacement of the points along the straight edge is defined by

$$u_z(h, y) = \frac{b_z}{\pi} \left(\theta - \frac{\pi}{2} \right), \quad \tan \theta = \frac{y}{b}. \quad (16)$$

The angle $\theta \in [0, \pi/2]$ for $y > 0$, and $\theta \in [3\pi/2, 2\pi]$ for $y < 0$ (Fig. 9a). The longitudinal displacement of the points along the boundary of the cavity is

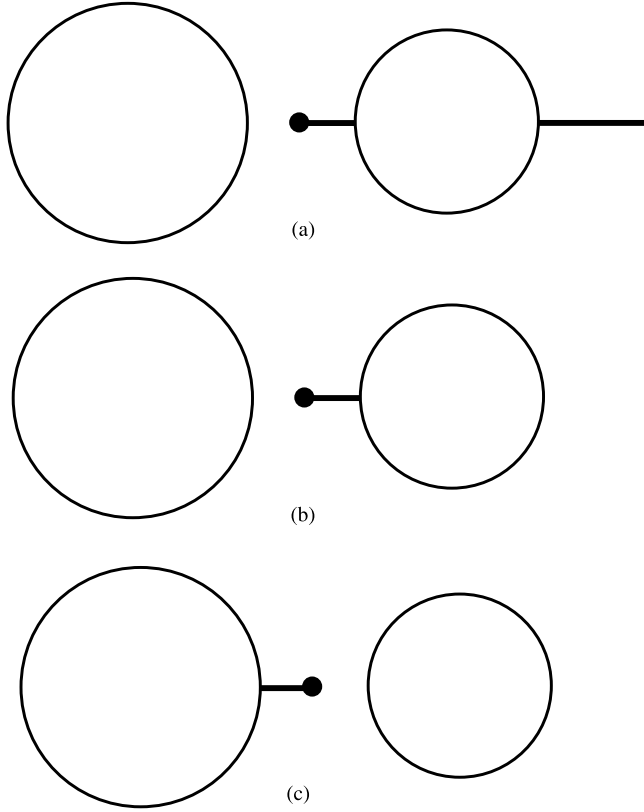


Fig. 7. Three different ways of creating a dislocation between two cavities in an infinite space by imposing a displacement discontinuity along one of the three indicated cuts.

$$u_z(R, \varphi) = \frac{b_z}{2\pi} (\theta_1 - \theta_2), \quad (17)$$

where the angles θ_1 and θ_2 are expressed in terms of the polar angle φ by using the relationships (Fig. 9b)

$$\sin\theta_{1,2} = \frac{R}{a_{1,2}} \sin\varphi, \quad (18)$$

$$a_{1,2}^2 = R^2 + (h \mp b)^2 - 2R(h \mp b)\cos\varphi.$$

These expressions can be conveniently used to determine the distortion of the bounding edges due to the imposed slip discontinuity along the width of the ligament.

A ligament in an eccentric hollow cylinder shown in Fig. 10. Since $R_1 = c + R_2 + d$, we can write

$$c = (R_1 - R_2)(1 - \zeta), \quad \zeta = \frac{d}{R_1 - R_2}. \quad (19)$$

The shear stress across the ligament is

$$\tau(x) = \frac{\mu b_z}{2\pi} \left(\frac{1}{x - x_2} - \frac{1}{x - x_1} \right). \quad (20)$$

The image dislocations needed to impose a displacement discontinuity across the ligament are approximately located at the distances

$$x_{1,2} = R_2 + R_1 \zeta \pm \sqrt{2R_1 R_2} \zeta^{1/2}, \quad (21)$$

from the center of the inner cylinder. The terms that are proportional to higher order exponents of the small ratio ζ are neglected in Eq. (21). The shear stresses at the end points of the ligament are then

$$\tau_1 = \tau(R_2) = \frac{\mu b_z}{\pi \sqrt{2R_1 R_2}} \left(1 + \frac{1}{2} \frac{R_1}{R_2} \zeta \right) \zeta^{-1/2},$$

$$\tau_2 = \tau(R_2 + d) = \frac{\mu b_z}{\pi \sqrt{2R_1 R_2}} \left(1 + \frac{1}{2} \frac{R_2}{R_1} \zeta \right) \zeta^{-1/2}. \quad (22)$$

This again establishes a $\zeta^{-1/2}$ order of singularity in the ligament, produced by the relative sliding of two faces of the ligament along the cut between the end points of the ligament. We retained the term proportional to ζ in Eq. (22) to quantify the difference between the shear stresses at the end points of the ligament. For instance, if $R_2 = 20b_z$, $c = 5b_z$, and $d = b_z$ (so that $\zeta = 1/6$), there follows $x_1 = 39.5b_z$, $x_2 = 11.17b_z$, $\tau_1 = 0.0268\mu$, and $\tau_2 = 0.0257\mu$.

Finally, consider a slip-induced stress amplification in the ligament between two cavities in an infinite medium (Fig. 11). Let d be a width of the ligament, so that

$$c = (1 + \rho + \zeta)R_1, \quad (23)$$

where

$$\rho = \frac{R_2}{R_1}, \quad \zeta = \frac{d}{R_1}. \quad (24)$$

The shear stress across the ligament is

$$\tau(x) = \frac{\mu b_z}{2\pi} \left(\frac{1}{x - x_1} - \frac{1}{x - c + x_2} \right). \quad (25)$$

The image dislocations needed to impose a displacement discontinuity across the ligament are approximately located at the distances

$$x_1 = \left[1 - \left(\frac{2\rho}{1 + \rho} \right)^{1/2} \zeta^{1/2} + \frac{\rho}{1 + \rho} \zeta \right] R_1,$$

$$x_2 = \left[\rho - \left(\frac{2\rho}{1 + \rho} \right)^{1/2} \zeta^{1/2} + \frac{1}{1 + \rho} \zeta \right] R_1, \quad (26)$$

from the centers of respective cavities. The terms that are proportional to higher order exponents of the small ratio $\zeta = d/R$ are neglected in Eq. (26). It readily follows that the shear stresses at the end points of the ligament are

$$\tau_1 = \tau(R_1) = \frac{\mu b_z}{\pi R_1} \left(\frac{1 + \rho}{2\rho} \right)^{1/2} \left(1 + \frac{1}{2} \frac{\rho}{1 + \rho} \zeta \right) \zeta^{-1/2},$$

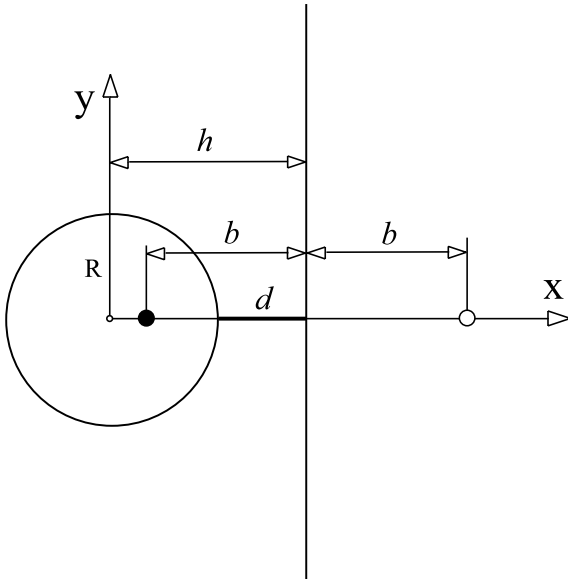


Fig. 8. Two image dislocations at the conjugate points needed to produce a slip discontinuity across the ligament of width d between a cavity and a free surface of a half-space.

$$\tau_2 = \tau(R_1 + d)$$

$$= \frac{\mu b_z}{\pi R_1} \left(\frac{1 + \rho}{2\rho} \right)^{1/2} \left(1 + \frac{1}{2\rho} \frac{1}{1 + \rho} \zeta \right) \zeta^{-1/2}, \quad (27)$$

which establishes a $\zeta^{-1/2}$ order of singularity in the region of thin ligament between two cavities in an infinite solid, produced by relative sliding of two faces of the ligament across its width. The terms proportional to ζ in Eq. (27) are retained to quantify the difference in the shear stresses at the end points of the ligament. If the cavities are identical ($R_1 = R_2 = R$), we obtain in the limit

$$x_1 = x_2 = (1 - \zeta^{1/2})R, \quad (28)$$

and

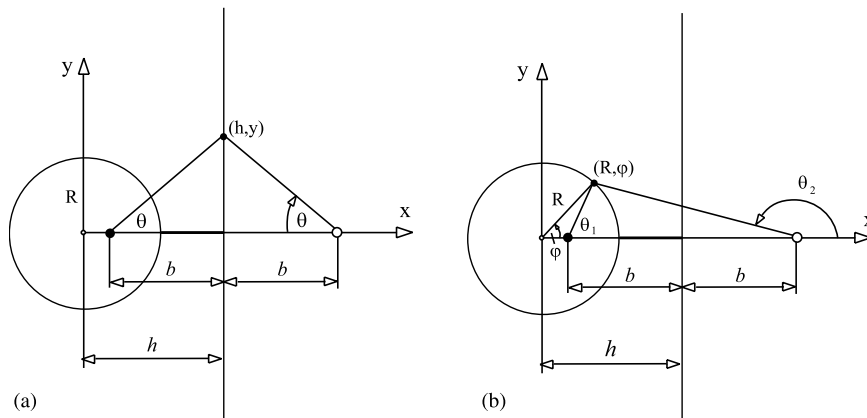


Fig. 9. The angles used in the expressions for the displacement along the straight edge and a boundary of the cavity due to the slip discontinuity from the cavity to the straight edge of a semi-infinite body.

$$\tau_1 = \tau_2 = \frac{\mu b_z}{\pi R} \zeta^{-1/2}. \quad (29)$$

Two numerical examples reveal the following. If $R_1 = 30b_z$, $R_2 = 10b_z$ and $d = 2b_z$, the image dislocations are approximately located at $x_1 = 25b_z$ and $x_2 = 4.98b_z$, while the shear stresses at the end points of the ligament are $\tau_2 = 0.0589\mu$ and $\tau_2 = 0.0625\mu$. The shear stress τ_2 is about 6% greater than τ_1 . In the case of two equal cavities of radius $R = 10b_z$ at the distance $d = b_z$, the image dislocations are located at $x_1 = x_2 = 7.34b_z$, while the shear stresses are $\tau_1 = \tau_2 = 0.1\mu$. If the cavities were at the distance $d = 10b_z$, the shear stresses would have been $\tau_1 = \tau_2 = 0.036\mu$. This is calculated from the exact results

$$x_1 = x_2 = \left[1 + \frac{1}{2} \zeta - \left(\zeta + \frac{1}{4} \zeta^2 \right)^{1/2} \right] R, \quad (30)$$

and

$$\tau_1 = \tau_2 = \frac{\mu b_z}{2\pi R} \left(1 + \frac{4}{\zeta} \right)^{1/2}. \quad (31)$$

In the limit of infinitely distant cavities the stress τ_1 approaches the value $\mu b_z / 2\pi R$, corresponding to a single dislocation at the origin.

6. Conclusions

We have presented in this paper the results for screw dislocations near cavities and straight boundaries, pointing out the differences in the solutions depending on the manner in which dislocations have been created. For example, three different solutions are derived for a screw dislocation between two cavities in an infinitely extended matrix. In general, for a dislocation in multiply connected region the solution is not unique, and depends on a cut used to create a dislocation. If the connectivity of the region is n , there are as many

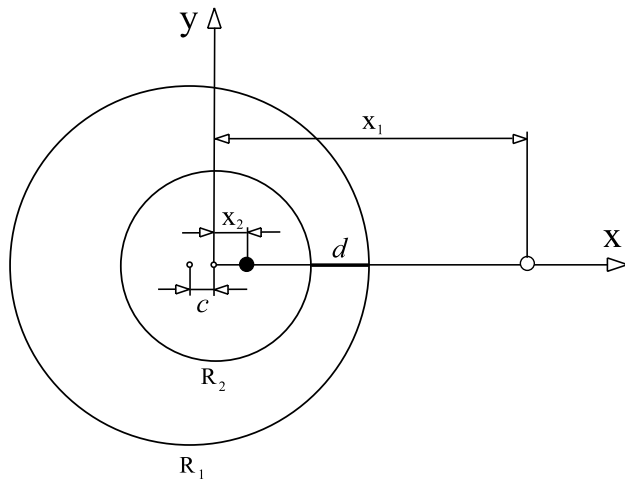


Fig. 10. Two image dislocations at the conjugate points needed to produce a slip discontinuity across the ligament of width d between the inner and outer boundaries of an eccentric hollow cylinder.

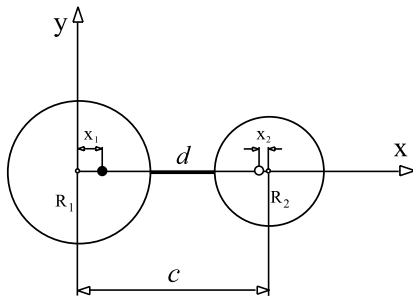


Fig. 11. Two image dislocations at the conjugate points needed to produce a slip discontinuity across the ligament of width d between two cavities in an infinite space.

possible solutions. The dislocation force and the equilibrium dislocation position have been determined in each considered case. We then provide an analysis of the slip-induced stress amplification in thin ligaments. For all considered geometries it is shown that the shearing stress amplifies at the order of $d^{-1/2}$ in the limit of vanishingly small ligament width d . Although the presented results

are derived for screw dislocations in antiplane strain, the obtained conclusions can be extended to edge dislocations in plane strain, albeit the latter analysis requires numerical evaluations based on the finite or boundary element method. This, as well as the stability analysis associated with a possible localized buckling of thin ligaments, is left for the future work.

Acknowledgements

V.A.L. is grateful for research support provided by the Montenegrin Academy of Sciences and Arts.

References

- [1] V.A. Lubarda, *J. Elasticity* 52 (1999) 289.
- [2] X. Markenscoff, *Comput. Mech.* 19 (1996) 77.
- [3] L. Wu, X. Markenscoff, *J. Mech. Phys. Solids* (1997) 2033.
- [4] J.D. Eshelby, *J. Appl. Phys.* 24 (1953) 176.
- [5] J.D. Eshelby, A.N. Stroh, *Phil. Mag.* 42 (1951) 1401.
- [6] F.R.N. Nabarro, *Theory of Crystal Dislocations*, Oxford University Press, Oxford, 1967.
- [7] J.P. Hirth, J. Lothe, *Theory of Dislocations*, second ed., Wiley, New York, 1982.
- [8] V.A. Lubarda, *J. Elasticity* 32 (1993) 19.
- [9] V.A. Lubarda, J.A. Blume, A. Needleman, *Acta Metall. Mater.* 41 (1993) 625.
- [10] V.A. Lubarda, D. Kouris, *Mech. Mater.* 23 (1996) 169.
- [11] V.A. Lubarda, D. Kouris, *Mech. Mater.* 23 (1996) 191.
- [12] V.A. Lubarda, *Int. J. Solids Struct.* 34 (1997) 1053.
- [13] V.A. Lubarda, *Math. Mech. Solids* 3 (1998) 411.
- [14] E.H. Yoffe, *Phil. Mag.* 6 (1961) 1147.
- [15] A.Y. Belov, in: V.L. Indenbom, J. Lothe (Eds.), *Elastic Strain Fields and Dislocation Mobility*, North-Holland, Amsterdam, 1992, pp. 391–446.
- [16] A. Seeger, in: S. Flügge (Ed.), *Handbuch der Physik, VII/1–Crystal Physics I*, Verlag, Berlin, 1955, pp. 383–665.
- [17] X. Markenscoff, V.A. Lubarda, In: M.A. Meyers, R.O. Ritchie (Eds.) *Microstructural Design of Advanced Materials*, Elsevier, 2003, in press.